



8th Manufacturing Engineering Society International Conference

Influence of the scanning strategy parameters upon the quality of the SLM parts

Sara Giganto^a, Pablo Zapico^a, M^a Ángeles Castro-Sastre^a, Susana Martínez-Pellitero^{a*},
Paola Leo^b, Patrizia Perulli^b

^aDepartment of Manufacturing Engineering, University of León. Campus de Vegazana, s/n. 24071 León. Spain

^bInnovation Engineering Department. University of Salento. La Stecca building, Via per Arnesano s.n., 73100. Lecce. Italy

Abstract

Nowadays, metal additive manufacturing techniques, such as Selective Laser Melting (SLM), are becoming more important due to their ability to manufacture very complex functional components. This ability is very interesting to industries as aerospace and automotive. Nevertheless, the installation of this techniques isn't as could be expected, mainly because of the high-quality requirements of the parts used in these industries. In this work the influence of several specific scanning strategy parameters and the post Heat Treatment (HT) used upon the microstructure and the hardness of the SLM parts have been analysed. For that, several stainless steel 17-4PH specimens were manufactured. Then, two different HTs were applied: stress relieving HT and stress relieving in combination with solution annealing and aging HTs. The hardness, microhardness and metallography general quality, were analysed for each specimen in order to determine the influence of the entire process in the quality of the parts.

© 2019 The Authors. Published by Elsevier B.V.

This is an open access article under the CC BY-NC-ND license (<http://creativecommons.org/licenses/by-nc-nd/4.0/>)

Peer-review under responsibility of the scientific committee of the 8th Manufacturing Engineering Society International Conference

Keywords: 17-4PH stainless steel; heat treatment; scanning strategy; SLM.

1. Introduction

Additive manufacturing (AM) is becoming increasingly important in almost all industrial sectors. Among AM techniques, Selective Laser Melting (SLM) stands out of them, because of its ability to manufacture metal parts with

* Corresponding author. Tel.: +034-987-291784; fax: +034-987-291930.

E-mail address: susana.martinez@unileon.es

relatively good mechanical properties, good enough for many actual applications, and without complex or expensive post-process procedures. As other AM techniques, SLM is able to produce very complex and personalized parts, but also in metallic materials, what is very interesting for industries such as aerospace and automotive. Nevertheless, several limitations in its implementation still exist today, which are mainly related to the lack of AM parts quality standardization and the high quality of parts required by these industries. So that, the analysis of the influence of various process and post-process parameters upon the SLM parts quality is today an important issue.

Several works about the analysis of SLM parts quality are focused in the influence of different process parameters, all of them related to the delivered laser energy to metal powders, like laser power, scanning speed, hatch distance, defocus, etc. Hu [1] studied the influence of separate SLM process parameters on the density, defect, microhardness and the influence of heat treatment (HT) on the mechanical properties of 17-4PH stainless steel. Ponnusamy [2] evaluated the influence of laser power, build orientation, layer thickness and laser defocus distance on the mechanical behaviour of SLM 17-4PH stainless steel parts under quasi-static compression. However, there are other parameters that have not been deeply analysed yet, such as used specific parameters for scanning strategy. During the manufacturing process, it's possible to use different scanning strategies to melt the powder bed, like normal, hexagonal or concentric strategy. Each strategy has its own parameters. The type of selected strategy and its setup have influence on the manufacturing time, as well as on the quality of the parts, what have been analysed in various works. Rashid [3] studied the effect of interlayer spacing scanning in different directions upon density and metallographic properties of 17-4PH parts, using normal strategy. Kudzal [4] evaluated the effect on microstructure and properties of additively manufactured 17-4PH stainless steel parts as a function of the scanning strategy (normal, hexagonal and concentric strategy). In order to achieve high density parts and good mechanical properties, hexagonal scanning strategy is recommended [4, 5].

Precipitation-hardened stainless steels, like 17-4PH, have been gaining importance as structural materials of small parts in several applications in aerospace and automotive industry, but also in others, such as chemistry and energy industries. 17-4PH steel combine high strength and good corrosion resistance. Furthermore, it has excellent mechanical properties at elevated temperatures, up to 300°C. Manufactured SLM parts of this material, have a yield strength of 620±30 MPa in as-built condition, being able to reach up to 1100±50 MPa after a proper HT post-process [6, 7]. In general, printed parts must be subjected to a stress relieving HT process before been separated from the build-up plate [8], to relieve thermal residual stresses induced during the printing process. This post-process HT allows to assure the geometrical quality of the part. A usual stress relieving HT for 17-4PH material consists of 650 °C for 2 hours and air cooling. Heat treatments influence the parts quality due to the important changes induced in the microstructure [9].

To date there is limited literature that studies the effect of different parameters of scanning strategy on the mechanical properties of 17-4PH SLM components analysing also the effect of the previous parameters in combination with a post-process HT. Therefore, in this work the influence in the quality of 17-4PH SLM parts of several specific scanning strategy parameters in combination with different recommended heat treatments procedures [10], has been analysed. For that, several specimens were analysed after building them with different parameters values of the hexagonal path scanning strategy and after post-treat them with different HTs (stress relieving and stress relieving in combination with solution annealing and aging), in order to relate the hardness, microhardness and microstructure to the entire process.

2. Equipment and Methodology

A SLM Metal 3DSystems ProX 100 machine (Table 1) was used to manufacture several parts with different scanning settings. Thirty specimens of 17-4PH Stainless Steel were manufactured from 3DSystems metallic powders (Table 2). Nitrogen, obtained from a generator connected to the machine, was used as inert gas during the manufacturing process.

Specimens manufactured by SLM were separated from the build-up plate by means of wire electrical discharge machining (WEDM). Then they were cut according to a transversal plane to the build direction by metallographic cutting machine. They were encapsulated and polished, in order to prepare the specimens for hardness, microhardness and microstructure analysis.

Table 1. ProX 100 features [11].

Property	Units	Value
Laser max Power	W	50
Laser Type	-	Fiber Laser
Laser Wavelength	nm	1070
Min Layer Thickness	μm	10
Preset Layer Thickness	μm	30
Repeatability X, Y, Z	μm	20, 20, 20
Typical Accuracy (min)	%	0.1-0.2 (50 μm)

Table 2. Chemical composition of 17-4PH powders [7].

Element	% of weight
Fe	Balance
Cr	15 – 17.5
Ni	3 – 5
Cu	3 – 5
Si	< 1.0
Mn	< 1.0
Nb	0.15 – 0.45

Hardness and microhardness tests have been carried out with a WIKI JS automatic hardness tester. A test load of 1 Kgf (equivalent to 9.807 N) to hardness HV1 and 100 gf (equivalent to 0.9807 N) to microhardness HV0.1 were applied for 15 seconds, according to Vickers Hardness UNE-EN ISO 6507 standard [12].

A Nikon Epiphot 200 microscope was used to capture optical micrographs following 5 seconds immersion in a solution of Behara etchant (distilled water, hydrochloric acid and potassium metabisulfite). The magnifications 200X and 1000X were used to take pictures of the analysed specimens.

X Ray diffraction analysis (XRD) was performed to clarify the microstructure of the SLM specimens. A Rigaku D/MAX-Ultima X-Ray system was employed for this analysis. Cu (K α) X-radiation was used.

2.1. Process and Scanning strategy parameters

This work focuses on the analysis of the influence of the scanning strategy parameters and not so much on the process parameters. The laser power and the defocusing parameters have been varied slightly to verify if their influence on the quality of the printed parts is comparable with the effect obtained by varying the scanning strategy parameters. Based on the results obtained from previous work [13], a starting point to vary the laser power and the defocusing parameters were established (38 W and 0 mm). In order to test little variations of these process parameters without disturb the quality of manufactured parts, they were varied as follows:

- Laser power parameter: 37.5 W, 38.5 W and 39 W.
- Defocusing parameter: -1 mm and +1 mm.

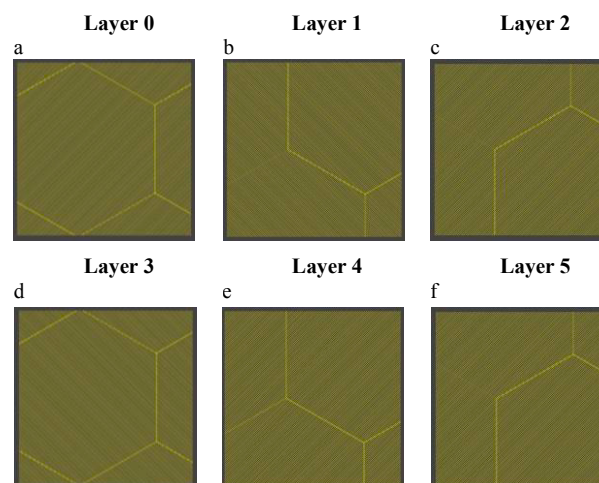


Fig. 1. Hexagonal pattern: (a) Position 1, direction 45°; (b) Position 2, direction -45°; (c) Position 3, direction 45°; (d) Position 1, direction -45°; (e) Position 2, direction 45°; (f) Position 3, direction -45°.

To reduce surface tensions generated during the melting process of the powder bed, hexagonal scanning strategy was used. This strategy divides each layer to be manufactured in hexagonal patches. Direction scanning paths change 45° to -45° in each layer. Moreover, the hexagonal pattern position changes each layer, repeating the same position every three layers. Layer 0, layer 1 and layer 2, are repeated successively, but with different scanning direction (Fig. 1). Layer 6 again matches with layer 0, both in the scan direction and in the hexagonal pattern position.

This scanning strategy allows the configuration of several parameters such as the radius, the overlap between hexagonal patches, the start and end of each scan path (back and forth), or the position sequence of this hexagonal patches between each layer (progress). Among these parameters, the radius and overlap are the most interesting ones to study. The radius parameter determines the size of the circles in which the hexagonal patches are inscribed. Fig. 2 shows graphically hexagonal scanning strategy parameters to study.

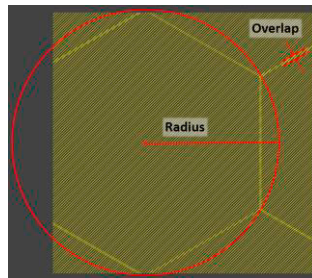


Fig. 2. Radius and overlap parameters of hexagonal scanning strategy.

Standard values of these hexagonal strategy parameters were taken as reference: 5000 μm of radius and 50 μm of overlap. In order to obtain the optimum setting of this strategy, radius and overlap parameters were varied within an acceptable range to right SLM manufacturing.

- Radius parameter: 2500 μm and 1250 μm .
- Overlap parameter: 75 μm and 25 μm .

2.2. Heat treatments

Due to the important changes induced in the microstructure of the SLM parts by different HTs applied after the manufacturing, in this work, the microstructural change and the difference in the hardness obtained by applying different heat treatments have been analysed, compared to as-built parts. For that, after the specimens were built, two different HTs were applied: stress relieving and stress relieving in combination with solution annealing and aging. Table 3 shows specifications heat treatments used.

Table 3. Heat treatments specifications.

HT	Temperature	Time	Cooling
Stress relieving	650 °C	2 h	air cooling
Solution annealing	1100 °C	1 h	air cooling
	+		
Aging	480 °C	1 h	air cooling

Thirty cubic specimens were manufactured. Ten were analysed as-built (C1-C10), another ten after the stress relieving treatment (C11-C20), and the other ten after the stress relieving, solution annealing and aging treatments (C21-C30). Specimen (C1), which was taken as reference, was manufactured according to the optimum settings of power and defocus and with the standard parameters of the hexagonal scanning strategy. The rest of specimens were manufactured with the same parameters as C1 but varying one of them. In this way, the influence of these parameters

can be studied independently. For example, in the case of specimens C2 and C3, the overlap parameter was varied. For specimens C4 and C5 the radius parameter was modified. On the other hand, the defocusing was varied in specimens C6 and C7. Finally, for specimens C8, C9 and C10 the laser power was varied. Table 4 shows a summary of manufacturing parameters considered in this paper with the used test nomenclature.

Table 4. Scanning parameters of specimens manufactured by SLM.

Parameter	Cubic Specimen									
	C1 (Reference)	C2	C3	C4	C5	C6	C7	C8	C9	C10
Laser Power (W)	38	38	38	38	38	38	38	37.5	38.5	39
Defocusing (mm)	0	0	0	0	0	-1	1	0	0	0
Radius (µm)	5000	5000	5000	2500	1250	5000	5000	5000	5000	5000
Overlap (µm)	50	25	75	50	50	50	50	50	50	50

3. Results and discussion

Small variations in the hardness of the different as-built specimens are observed (C1-C10) with respect to the reference part (Fig. 3a). This is justified by the few differences found in the microstructure. The hardness value of the reference specimen C1 is 274 HV1. The range of difference are from 262 HV1 in the case of specimen C6 (that has a defocusing value of -1 mm) to 306 HV1 corresponding to specimen C2 (that has an overlap value of 25 µm) as shown in Fig. 3a.

Regarding the effect of the scanning strategy parameters, decreasing the radius decreases the hardness. Instead, the overlap doesn't indicate a clear trend and it would be desirable to extend the study to wider ranges relative to the reference value.

Regarding the process parameters, the effect of its slight variation is similar to that produced by the variation of the scanning strategy parameters (Fig. 3a). In this study it is observed as small variations in the defocusing parameter produce large variations in hardness relative to the reference value, especially when this parameter decreases. In contrast, small variations in the power parameter don't show significant variations in the hardness value. It can be concluded that these process parameters, and the small variations that could be made in them, do not provide relevant information regarding their effect on the hardness of the printed parts. Higher variations in the laser power and defocusing parameters would probably produce higher differences in hardness, but would go against the quality of the printed parts.

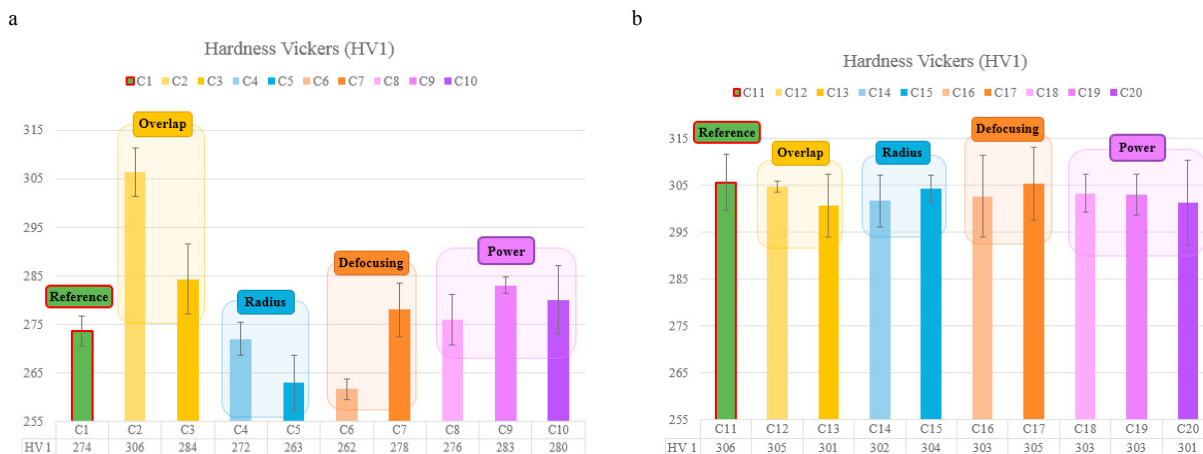


Fig. 3. (a) Hardness Vickers of as-built specimens; (b) Hardness Vickers of stress relieving specimens.

Hardness variations observed between the specimens built with different process and scanning strategy parameters disappears after heat treatments as shown in Fig. 3b. After stress relieving treatment, the hardness increases slightly around 303 HV, while the variations observed between specimens manufactured with different parameters disappear (Fig. 3b).

Instead, as expected, the aging HT results in a considerable increase in hardness, which reaches values of 405 HV (Fig. 4). As in the stress relieving HT, the hardness remains practically constant for any parameter studied in this work. This demonstrates the independence of the studied parameters in the hardness obtained by any of the HTs analysed here.

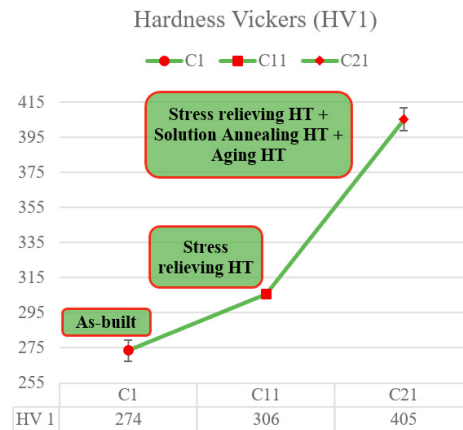


Fig. 4. Hardness Vickers of reference specimen with the different post-treatments.

Regarding the microstructure, no changes were observed with different parameters, but significant differences were observed applying different HTs. The microstructure of the as-built specimens in the transversal plane to the build direction is characterized by footprints of laser track visible as parallel line (Fig. 5a). The solidified grains in the melt pool are mainly columnar while at the pool boundary a mixed microstructure containing fine and equiaxed grains have been observed. The XRD pattern for the transversal plane (Fig. 5b) shows the presence of both martensitic or ferritic α phase and austenitic γ phase. In fact, because of the very low carbon concentration in this alloy, the magnitude of the lattice distortion in the body-centred tetragonal (BCT) martensite is very small and it is not possible to distinguish between the body centred cubic (BCC) ferrite and the BCT martensite [14]. As such the specimen microstructure could contain both ferritic/martensitic microstructure (usually observed in the 17-4PH stainless steel) together with retained austenite, due to the high-density energy process that promotes a significant metastability.

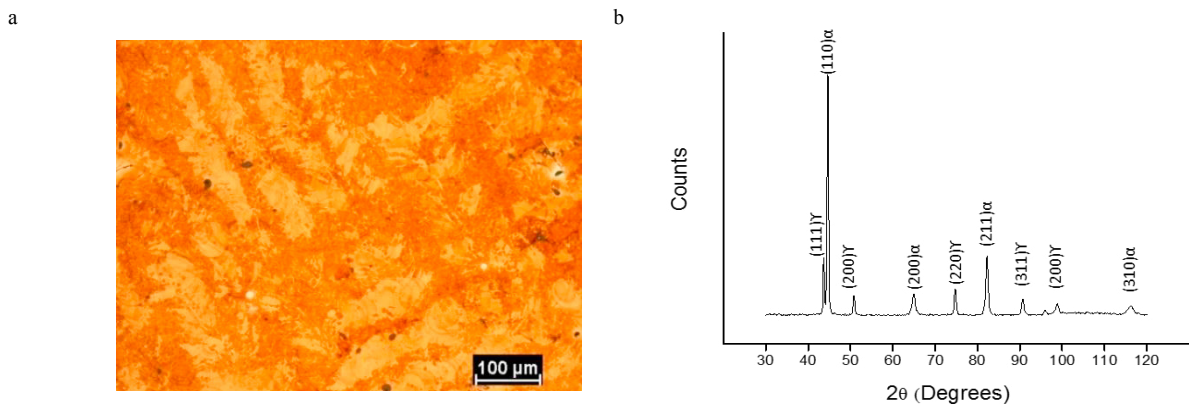


Fig. 5. (a) Microstructure of as-built specimen C1 (magnification 200X); (b) XRD pattern for the transversal plane of C1 specimen.

After stress relieving HT a slight increase in hardness (Fig. 4) has been observed probably due to heterogeneous nucleation and growth of particles or to a reduction in austenite phase fraction at room-temperature [10]. As expected, the specimens submitted to aging HT exhibit the highest hardness (Fig. 4) due to both martensitic microstructure and precipitated hard particles. Fig. 6 shows the microstructure of the reference specimen in the three different states analysed: as-built (Fig. 6a), with stress relieving HT (Fig. 6b), and with stress relieving, solution annealing and aging HTs (Fig. 6c).

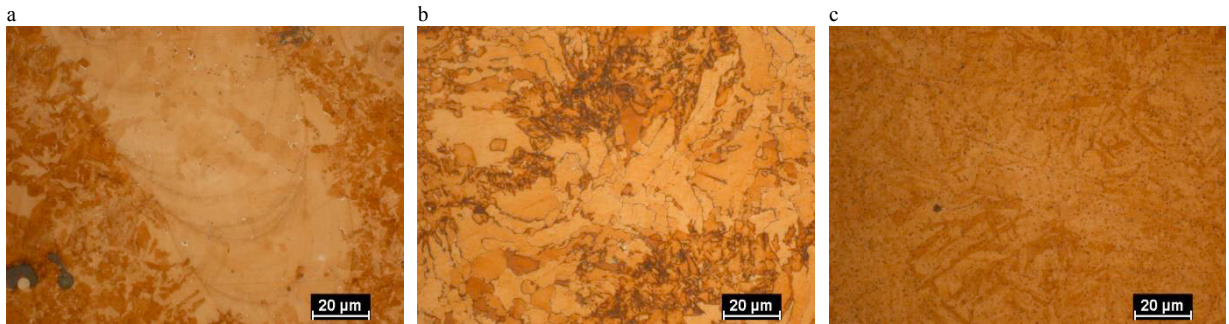


Fig. 6. Microstructure of: (a) as-built specimens C1; (b) stress relieving HT specimens C11; (c) stress relieving, solution annealing and aging HTs specimens C21.

4. Conclusions

In this work, the influence in the hardness of 17-4PH SLM parts, with several specific scanning strategy parameters in combination with different heat treatments procedures, has been analysed. Based on the results obtained from previous works, a reference specimen with certain process parameters was established. According to SLM manufacturer's recommendations, hexagonal scanning strategy was used. The standard parameters of these strategy were set for the reference specimen. In order to quantify the influence of these parameters, radius and overlap parameters were varied within an acceptable range to right SLM manufacturing. In addition, two different HTs (stress relieving and stress relieving in combination with solution annealing and aging) were studied.

Regarding hardness analysis, there are slight variations of hardness between the as-built specimens manufactured with different scanning strategy parameters. However, these variations disappear after stress relieving HT.

Microstructure shows no relevant differences between specimens built with different scanning strategy parameters. Unlike the traditional microstructure for 17-4PH specimen containing Ferrite and Martensite, the SLM microstructure of the as-built specimens characterized in this study exhibits also austenitic phase due to the high-density energy process that promotes a significant metastability.

However, there are variation between the different post-treatments applied. After stress relieving HT a slight increase in hardness has been observed probably due to heterogeneous nucleation and growth of particles or to a reduction in austenite phase fraction at room-temperature. As expected, the specimens submitted to solution annealing and aging HTs exhibit the highest hardness due to both martensitic microstructure and precipitated hard particles.

Regarding the influence of these parameters on the parts hardness, it would be appropriate to extend this study in order to find the appropriate parameters of overlap and radius to optimize the printing process (in terms of time and cost), as the need for subsequent treatments, homogenize the values of hardness achieved.

Acknowledgements

We gratefully acknowledge the financial support provided by the Junta de Castilla y León and FEDER (project LE027P17) and by the Spanish Ministry of Economy, Industry and Competitiveness (project DPI2017-89840-R). We also gratefully the Grupo Hedisa collaboration in the development of this research.

References

- [1] Z. Hu, H. Zhu, H. Zhang, X. Zeng, Experimental investigation on selective laser melting of 17-4PH stainless steel, *Optics & Laser Technology*, 87 (2017) 17-25.
- [2] P. Ponnusamy, S. H. Masood, D. Ruan, S. Palanisamy, R. A. Rahman Rashid, O. A. Mohamed, Mechanical performance of selective laser melted 17-4 PH stainless steel under compressive loading, *Proceedings of the 28th Annual International Solid Freeform Fabrication Symposium - An Additive Manufacturing Conference*, (2017) 321 - 331.
- [3] R. Rashid, S. H. Masood, D. Ruan, S. Palanisamy, R. A. Rahman Rashid, M. Brandt, Effect of scan strategy on density and metallurgical properties of 17-4PH parts printed by Selective Laser Melting (SLM), *Journal of Materials Processing Technology*, 249 (2017) 502-511.
- [4] A. Kudzal, B. McWilliams, C. Hofmeister, F. Kellogg, J. Yu, J. Taggart-Scarff, J. Liang, Effect of scan pattern on the microstructure and mechanical properties of Powder Bed Fusion additive manufactured 17-4 stainless steel, *Materials & Design*, 133 (2017) 205-215.
- [5] R. Rashid, S. H. Masood, D. Ruan, S. Palanisamy, R. A. Rahman Rashid, J. Elambasseril, M. Brandt, Effect of energy per layer on the anisotropy of selective laser melted AlSi12 aluminium alloy, *Additive Manufacturing*, 22 (2018) 426-439.
- [6] W. D. Yoo, J. H. Lee, K. T. Youn, Y. M. Rhyim, Study on the Microstructure and Mechanical Properties of 17-4 PH Stainless Steel depending on Heat Treatment and Aging Time, *Solid State Phenomena*, 118 (2006) 15-20.
- [7] 3DSystems (2017), *LaserForm 17-4PH (B) for ProX DMP 100, 200 and 300 Direct Metal Printers*.
- [8] T. M. Mower, M. J. Long, Mechanical behavior of additive manufactured, powder-bed laser-fused materials, *Materials Science & Engineering A*, 651 (2016) 198-213.
- [9] C. N. Hsiao, C.S. Chiou, J. R. Yang, Aging reactions in a 17-4 PH stainless steel, *Materials Chemistry and Physics*, 74 (2002) 134-142.
- [10] S. D. Meredith, J. S. Zuback, J. S. Keista, T. A. Palmer, Impact of composition on the heat treatment response of additively manufactured 17-4PH grade stainless steel, *Materials Science & Engineering A*, 738 (2018) 44-56.
- [11] 3DSystems (2017). *Direct Metal Printers. Metal Additive Manufacturing with the ProX DMP 3D printers*.
- [12] ISO 6507-1: *Metallic materials -- Vickers hardness test -- Part 1: Test method* (2018).
- [13] P. Zapico, S. Giganto, S. Martínez-Pellitero, A. I. Fernández-Abia, M. A. Castro-Sastre, Influence of laser energy in the surface quality of parts manufactured by selective laser melting, *Proceedings of the 29th DAAAM International Symposium* (2018).
- [14] Y. Sun, R. J. Hebert, M. Aindow, Effect of heat treatments on microstructural evolution of additively manufactured and wrought 17-4PH stainless steel, *Materials & Design*, 156 (2018) 429-440.